Differential effects of macronutrient content in 2 energy-restricted diets on cardiovascular risk factors and adipose tissue cell size in moderately obese individuals: a randomized controlled trial[1–4]

Salwa W Rizkalla, Edi Prifti, Aurélie Cotillard, Veronique Pelloux, Christine Rouault, Reginald Allouche, Muriel Laromiguière, LingChun Kong, Froogh Darakhshan, Florence Massiera, and Karine Clement

ABSTRACT

Background: The most effective and safe dietary approach for weight loss and its impact on the metabolic functions and morphology of adipose tissue remain unclear.

Objectives: We evaluated whether an energy-restricted high-protein diet with a low glycemic index and soluble fiber (LC-P-LGI) would be more effective than a low-calorie conventional diet (LC-CONV) on weight loss and related metabolic risk factors. We further determined factors that may influence adipocyte size during energy restriction.

Design: Thirteen obese participants were randomly assigned in a crossover design to 2 periods of a 4-wk hypocaloric diet as either LC-P-LGI or LC-CONV, separated by 8-wk washout intervals.

Results: In comparison with the LC-CONV diet, the main effect of the LC-P-LGI diet was a greater decrease in adipocyte diameter (P = 0.048), plasma plasminogen activator inhibitor protein-1 (P = 0.019), vascular endothelial growth factor (P = 0.032), and interferon-γ inducible protein 10 (P = 0.010). Whereas fasting plasma glucose and high-sensitivity C-reactive protein decreased only after the LC-P-LGI diet, with no differences between diets, fasting plasma insulin and insulin resistance were lower after the LC-CONV diet. The diet results did not differ for body composition and lipid variables. Kinetic modifications in adipocyte diameter were associated with metabolic variables and genes implicated in adipocyte proliferation, apoptosis, and angiogenesis.

Conclusions: In comparison with the LC-CONV diet, the LC-P-LGI diet was associated with improvement in some cardiometabolic risk factors and greater reduction in adipocyte size. Profiles of genes involved in inhibiting adipogenesis and angiogenesis, but increasing apoptosis, were correlated with decreased adipocyte size. This study provides insight into the adipose tissue–remodeling changes that induce regulation of adipocyte size during dietary weight loss. This trial was registered at clinicaltrials.gov as NCT01312740. *Am J Clin Nutr* 2012;95:49–63.

INTRODUCTION

A vigorous debate exists with regard to the optimal dietary macronutrient composition that would facilitate weight loss with safety and that would promote weight maintenance. A substantial decrease in fat intake with a compensatory increase in carbohydrates has been first adopted. This strategy was criticized because, although 5–7 kg weight loss could be obtained, subsequent weight regain could not be avoided in the long term (1).

High-protein diets are considered to be more effective for weight loss and weight maintenance than other diets because of their satiating and thermogenic effects (2). The quality of carbohydrates with a LGI[5] also was proposed to offer additional benefit. It might indeed positively affect satiety and fat oxidation at the expense of carbohydrate oxidation (3). Another component is the fiber content of the diet. High fiber intake was associated with lower weight gain than with other diets (4). This outcome raises the question about the most effective dietary approach for weight loss without potential adverse effects or transient outcomes. Recently, in the Diet, Obesity, and Genes (DIOGENES) trial, whereas variations in macronutrients had no major effect on weight loss, better weight maintenance was achieved with a modest increase in protein content and a reduction in the glycemic index of the diet (5).

---

[1] From INSERM, U872, Nutriomique Team 7, and the Université Pierre et Marie Curie-Paris 6, Centre de Recherche des Cordeliers, UMR S 872, Paris, France (SWR, AC, VP, CR, LK, FD, and KC); the Assistance Publique-Hôpitaux de Paris, ICAN (Institut de Cardiometabolism & Nutrition), Nutrition and Endocrinology Department Pitié-Salpêtrière Hospital, and the Centre de Recherche Nutrition Humaine, Ile de France, Paris, France (SWR, LK, FD, and KC); the Biochemistry Laboratory, Hotel Dieu Hospital, Paris, France (ML); and the CEPRODI-KOT Laboratory, Paris, France (RA and FM).

[2] Part of this study was presented at the 70th Scientific Sessions of the American Diabetes Association, Orlando, FL, 25–29 June 2010.

[3] Supported by grants from CEPRODI-KOT Laboratory (European Company of Diet Products designing nutritional intervention strategies based on innovative food products for weight management), INSERM, University Pierre and Marie-Curie, Paris, France, and Region Ile de France [CODDIM (cardiovascular-obesity-diabetes as a "domain d'intérêt majeur") to KC and FD)].

[4] Address correspondence to SW Rizkalla, Department of Nutrition, INSERM U872, CRNH-Ile de France, Batiment Benjamin Delessert, Hopital Pitié Salpêtrière, 82 Boulevard de l'Hopital, Paris, France 75013. E-mail: salwa.rizkalla@psl.aphp.fr.

[5] Abbreviations used: G-CSF, granulocyte colony-stimulating factor; GO, Gene Ontology; HOMA-B, B cell function; HOMA-S, insulin sensitivity; hs-CRP, high-sensitivity C-reactive protein; IFN-γ, interferon γ; IP-10, interferon-γ inducible protein 10; LC-CONV, low-calorie conventional diet; LC-P-LGI, low-calorie, high-protein, low–glycemic index diet; LGI, low glycemic index; MIP-1A, macrophage inflammatory protein 1A; MIP-1B, macrophage inflammatory protein 1B; PAI-1, plasminogen activator inhibitor protein-1; PDGF, platelet-derived growth factor; RT-PCR, reverse transcriptase–polymerase chain reaction; VEGF, vascular endothelial growth factor.

Received April 4, 2011. Accepted for publication October 19, 2011.

Nevertheless, data remain scarce with regard to the influence of macronutrient composition on adipose tissue biology and structure during a hypocaloric program. Adipose tissue is an important metabolic organ that has the capacity to store and release energy when needed. This tissue also links obesity to its numerous comorbidities via the secretion of a large panel of molecules, some of them are considered to be metabolic and cardiovascular risk factors. Subcutaneous adipose tissue gene expression has been shown to be a useful tool for reflecting molecular adaptations to different dietary programs (6). By using gene expression profiling (7), we previously described the modulation of several inflammatory genes induced by energy restriction and showed that many inflammatory genes were expressed in cells of the stromal vascular fraction. The association between gene expression changes in adipose tissue and the modification of adipocyte size, an important obesity-related phenotype, has not been explored kinetically in moderately obese individuals. In morbid obesity, adipose tissue hyperplasia with many small adipocytes is mainly associated with better glucose, insulin, and lipid profiles than is adipose tissue hypertrophy with large adipocytes (8). Obesity-associated hypertension may also be causally related to the accumulation of large adipocytes (9).

Moreover, to our knowledge no current study has investigated the effect of macronutrient composition in a hypocaloric diet on adipose tissue gene expression and its relation to adipocyte size kinetic changes.

Therefore, we designed this study to evaluate whether a low-calorie (1200 kcal/d), low-fat diet compensated by proteins and with carbohydrates of LGI and soluble fiber (LC-P-LGI diet) might provide a possible approach to achieving better metabolic and weight-reduction benefits than a low-calorie conventional diet (LC-CONV diet). We further characterized the adipose tissue gene expression profile during the entire dietary intervention and identified genes that are primarily associated with adipocyte size modulation.

SUBJECTS AND METHODS

Participants and study design

Participants

The participants were recruited at the outpatient clinic of the Nutrition Division, Hôtel-Dieu Hospital, Paris, France. We excluded from the study patients with abnormalities of renal, hepatic, or thyroid function or with gastrointestinal disorders ($n = 5$). Fourteen individuals who met the following criteria were initially included: age 30–60 y, BMI (in kg/m^2) between 27 and 38, and fasting plasma glucose <6.5 mmol/L. None of the participants were receiving treatment for chronic diseases or had been involved in weight-loss programs in the preceding 12 mo. Individuals following a vegetarian diet were not included. Clinical and biological characteristics of the participants are shown in **Table 1**. The sample size was calculated after fixing the probability of a type 1 error at 0.05 and that of a type 2 error at 0.10 for fat mass changes of 5–7% (10). During the follow-up, one patient was excluded from the study because of poor compliance with the dietary recommendations. A physician explained the purpose, nature, and potential risks of the study; and each patient provided written informed consent. The experimental protocol was approved by the ethics committee of Hôtel-Dieu Hospital, Paris.

TABLE 1
Clinical characteristics of the subjects at the time of screening[1]

	Value
Sex (*n*)	5 F/8 M
Age (y)	45.0 ± 2.4[2]
Body weight (kg)	91.98 ± 3.38
BMI (kg/m^2)	31.86 ± 1.30
Fasting plasma glucose (mmol/L)	4.98 ± 0.14
Plasma triacylglycerol (mmol/L)	1.60 ± 0.25

[1] $n = 13$.
[2] Mean ± SEM (all such values).

Study design

The participants (8 men and 5 postmenopausal women) were randomly allocated in a crossover design to 2 periods of 4 wk of an energy-restricted diet containing 1200 kcal as either a conventional diet (LC-CONV) or as a special energy-restricted diet compensated by protein (LC-P-LGI). The 2 nutritional periods were separated by a washout interval of 8 wk. Before the start of the study, participants were instructed to maintain their usual lifestyle during the experimental period.

At the beginning (day 0) and the end (week 4) of each dietary period, participants underwent a series of tests after an overnight fast. Thirty minutes after arrival, a sample of subcutaneous abdominal adipose tissue was obtained by needle biopsy by using a 14-gauge needle under local anesthesia with Xylocaine 10% without adrenaline (AstraZeneca). Two samples of adipose tissue were also taken 5 d after the start of each dietary period to examine early gene expression changes. A fresh aliquot (10 μL sample) was collected to measure adipocyte diameter. The remaining portion (500–800 mg) was immediately frozen in liquid nitrogen and stored at −80°C for subsequent RNA extraction, microarray studies, and real-time RT-PCR analysis.

An indwelling catheter was then inserted into a vein in the cubital fossa for blood sampling. After a fasting blood sample was taken, an oral-glucose-tolerance test was performed with blood samples taken at 30, 60, 90, and 120 min after 75 g glucose ingestion.

Blood samples were centrifuged immediately, and plasma was separated and frozen at −20°C for measurement of plasma lipids (total cholesterol, HDL cholesterol, and triglycerides), insulin and glucose values, leptin, adiponectin, and inflammatory markers [eg, hs-CRP, IL-6, and other inflammatory and cardiovascular risk markers (PAI-1, VEGF)].

Body fat and fat-free mass distributions were measured by using dual-energy X-ray absorptiometry (GE Lunar Prodigy Corporation) before and after each dietary period.

Dietary follow-up

At the start of the study, participants received individual counseling from a registered dietitian who also monitored each individual during the different phases. Dietary intake was prescribed individually according to information obtained from dietary questionnaires (3-d recall technique) at the beginning of the study. The 4-wk LC-P-LGI period consisted of the participants' consumption of a hypocaloric diet based on a strictly controlled amount of 1200 kcal/d (35% protein, 25% lipids, and 40% carbohydrates). This diet consisted of habitually consumed foods that were supplemented daily with 4 dietary products (60–75 kcal; designed by CEPRODI-KOT Laboratory). These supplements consisted of lyophilized powder enriched in protein and soluble fiber (mainly inulin) and composed of LGI carbohydrates. The composition of these conditioned-powder supplements was prepared as described in Supplementary Table 1 under "Supplemental data" in the online issue. The supplements were included in the daily menu, as shown in Supplementary Table 2 under "Supplemental data" in the online issue, which consisted of a hypocaloric diet low in lipids (25%) and compensated by protein (35%) with no change in carbohydrate content.

The 4-wk LC-CONV period consisted of a 1200-kcal/d diet (25% protein, 31% lipids, 44% carbohydrates). During the 8-wk washout period, the participants were instructed to increase their caloric intake slightly (+20% kcal of their calculated energy expenditure) to stabilize their body weight.

Patients were asked to complete a 7-d food diary just before the start of each dietary period. To determine compliance with the dietary recommendations, the patients were asked to complete another food diary that was filled in during the last 7 d of each period. Even if the 7-d food diary record was not able to exclude underestimation of total food intake, we could compare the declared food consumption before and after each dietary treatment period. All records were analyzed by a registered dietitian by using the computer software program PROFILE DOSSIER V3 (Audit Conseil en Informatique Médicale), which has a dietary database made up of 400 food items or groups of foods representative of the French diet as described previously (11). The compositions of dietary supplements used in the LC-P-LGI diet and of any uncharted food were also added to the database.

Insulin-sensitivity measurements

Estimations of pancreatic β cell function (insulin secretion) and insulin sensitivity were calculated from fasting plasma insulin and glucose measurements by using homeostasis model assessment HOMA/CIGMA software (12).

Adipocyte morphology

One small portion of the subcutaneous adipose tissue biopsy samples was immediately isolated by collagenase digestion according to the method described in reference 13. In brief, ~40–50 mg adipose tissue were rapidly washed with physiologic saline and then incubated with collagenase (1 mg/mL) in 500 μL phosphate buffer saline (Sigma) solution (pH 7.4) at 37°C for 20 min. Adipocytes were then rapidly washed 3 times with physiologic saline at 37°C to eliminate all traces of collagenase. For cell size measurements, an aliquot of adipocyte suspensions was placed in a circular silicone artisan ring (0.5 cm diameter) that was fixed to a silicon glass slide, to limit the dispersion of the adipocyte suspension, then visualized under a light optic microscope attached to a camera and computer interface. Adipocyte diameters were measured with PERFECT IMAGE software (Numeris). Mean diameter was defined as the mean value for the distribution of adipocyte diameters of 150 cells.

Microarray experiments

Subcutaneous adipose tissue samples were obtained by needle aspiration after an overnight fast before each dietary period, at day 5, and at the end of each dietary period. We therefore collected at 6 time points: day 0, day 5, day 30 (end of the first period), day 90 (day 0 of second period), day 95, and day 120 (end of the second period). Samples were stored at −80°C until they were further processed for microarray and RT-PCR analysis. Total RNA was extracted by using the RNeasy total RNA Mini kit (QIAGEN) with one-column DNase digestion. RNA quality and concentration were assessed by using an Agilent 2100 Bioanalyzer (Agilent Technologies).

Gene expression experiments were performed in 10 participants throughout the entire study duration (ie, 6 time points: day 0, day 5, day 30, day 90, day 95, and day 120), leading to the creation of 60 individual complementary DNA microarrays. Subjects who had a missing time point or who had degraded samples were eliminated. An Illumina RNA amplification kit (Ambion) was used according to the manufacturer's instructions to obtain biotin-labeled complementary RNA from 250 ng total RNA. This amplification procedure is well validated and does not distort the relative abundance of individual messenger RNAs within an RNA population.

Hybridization processes were performed with Illumina Human HT-12 version 3.0 Expression BeadChips (Illumina Inc), which contain probes for 48,000 transcripts. Twelve samples were screened simultaneously in each chip. Hybridized probes were detected with cyanin-3-streptavidin (1 mg/mL; Amersham Biosciences, GE Health Care) and scanned by using an Illumina BeadArray Reader.

Raw data were extracted with Illumina BeadStudio version 3.0.19 software by using the default settings and without any additional normalization. The background for each bead was computed as the mean of the 5 dimmest pixels in the area around the given bead. Outliers of transcript replicates >3 SDs from the replicate median were removed. The raw microarray data are available for download at the Gene Expression Omnibus public repository (access link number: GSE27121).

Analysis of the biological interactions characterizing the transcriptomic signature of the 2 energy-restricted diets

The strategy applied to analyze differentially regulated genes consisted of 3 consecutive steps: *1*) identification of contextually relevant biological themes through an automated annotation of the genes whose expression was regulated by the energy-restricted diets, *2*) quantification of the transcriptomic interactions relating relevant biological themes and construction of functional interaction maps characterizing the transcriptomic signature of the genes discriminated by the diets, and *3*) analysis of the gene coexpression networks underlying the biological interaction modules and computation of network centrality measures for related gene nodes.

Biological annotation of energy-restriction-modulated genes

An automated annotation procedure of the genes whose expression was modulated during the entire dietary intervention was performed by using the FunNet tool (http://www.funnet.info). This procedure has been extensively described elsewhere (14, 15).

Analysis of functional interactions between overrepresented biological themes

The analysis of functional interactions aimed to extract relevant information about the complex relations between various structural and functional themes in subcutaneous adipose tissue during the dietary intervention. This approach used information about similarities between gene expression profiles and the subsequent significantly enriched GO categories as explained in the first step. A comprehensive map showing the interactions between biological themes that characterize the transcriptomic signature of the energy-restricted dietary intervention was also computed as described elsewhere (14).

Analysis of the coexpression network

Coexpression network analysis was performed to relate annotated genes whose expression was modulated by the entire energy-restricted dietary intervention with relevant biological themes. The analytic framework used to construct the networks of coexpressed genes was described in Zhang and Horvath (16). Spearman's correlation coefficient was used to quantify the similarity among gene expression profiles and to obtain a coexpression matrix. Then, an adjacency matrix was computed by applying a "hard" threshold parameter of 0.5 to the coexpression matrix. This value was determined by maximizing a scale-free topology criterion as previously described (16).

Microarray data confirmation

To confirm the results obtained by microarray experiments, we compared the expression profiles of a subset of significantly modulated genes by using a large-scale RT-PCR performed with the use of Fluidigm (http://www.genomeweb.com/arrays/fluidigm-integragen-form-french-alliance). First-strand complementary DNA was synthesized from 500 ng total RNA obtained from adipose tissue biopsy samples with 100 units of Superscript II (Invitrogen) by using oligo (dT) primers and random hexamers (Promega). Validation of the microarray analysis is presented in Supplementary Figure 1 and Supplementary Table 3 under "Supplemental data" in the online issue.

Biochemical assays

Plasma glucose was measured by the glucose oxidase method (Beckman Fullerton). Plasma insulin was determined by using an immunoenzymatic automatic system (Access Immunoassay System; Beckman Coulter). Plasma triacylglycerols were measured with Biomérieux kits; and total, HDL, and LDL cholesterol were measured with Labintest kits. Plasma PAI-1 was measured with Chromolize/PAI-1 kits (Biopool International). Leptin and adiponectin were determined by using ELISA kits from R&D Systems Europe. Other inflammatory markers [eosinophil-selective chemoattractant chemokine (eotaxin); G-CSF; interferon-γ, PDGF, IP-10, MIP-1A and -1B), TNF-α, and VEGF] were measured by using the human cytokine multiplex panel kits (Bio-Rad). A multiplex assay was performed according to the manufacturer's instructions. Multianalytic profiling was performed with the Luminex-200 system and the Xmap Platform (Luminex Corporation). Acquired fluorescence data were analyzed by using Xponent software, with standard curves obtained from serial dilutions of standard cytokine mixtures. Serum samples were diluted (1:4). Plasma cystatin C and creatinine were measured to evaluate renal function. Cystatin C was measured by means of a particle-enhanced immunonephelometric assay (N Latex Cystatin C; Dade Behring) with a nephelometer (BNII; Dade Behring).

Statistical analysis

Clinical variables

The validity of the crossover design was tested by ANCOVA of baseline results of the second period, with baseline results of the first period accounting as the covariable and the diet of the first period as the main factor.

The effects of the 2 diets were compared by using a MANOVA (multivariate analysis of repeated measurements) with 2 within-subject factors: diet and time. Because some baseline values were significantly different between the 2 dietary arms before the start of each specific diet (as for adipocyte diameter, glycemia, and VEGF), baseline values were treated as outcomes, rather than as model covariates. The primary hypothesis compared the delta (Δ) changes during each dietary period (Δ4 wk – baseline values in LC-P-LGI compared with LC-CONV) by examination of the diet × time interaction. Changes during each dietary period (4 wk compared with baseline results) were also reported; however, differences between diets were interpreted only when the diet × time interaction was significant (diet effect). For significant variables, the percentage changes during the 4-wk dietary period were also estimated and compared. Results were considered significant when $P < 0.05$. These analyses were carried out by using JMP, version 9, statistical software (SAS Institute Inc). Data are expressed as means ± SEMs.

Gene expression analysis

Statistical analysis of microarray data was performed with the R software environment for statistical computing (R Development Core Team 2010), including Bioconductor packages (17). The raw expression data for each microarray were quantile-normalized with the "lumi" package (18). We used SAM software (Significance Analysis of Microarray, version 3.09, available at http://www.stat.stanford.edu/tibs/SAM/) to identify the genes whose expression varied with time through the "one class time" method. Similarly, we used SAM to identify the genes whose expression discriminated between the 2 diets (diet effect) with the "2 class paired" method and finally to identify genes whose expression discriminated between the 2 dietary periods comprised in this study (period effect) with the "2 class unpaired time" method. In all 3 analytic cases, the option "slope" was selected. Only the genes with a false discovery rate <5% were retained for further analyses.

Correlation analysis

Relations between variables were analyzed by using Pearson or Spearman correlation according to the number of observations, and *r* or rho coefficients were provided. Adjustments by fat mass percentage were performed by using partial correlations. In all conditions in which multiple testing errors were expected because of the high number of consecutive statistical computations, the *P* values computed from the aforementioned tests were adjusted. For the gene analysis, a *q*-value adjustment using the R qvalue package (available at http://www.R-project.org) (19) was used. For the analysis of clinical variables, a Benjamini-Hochberg adjustment (20) was used. This choice was motivated by the existence of a high proportion of significant P values (<0.05). We used a threshold corresponding to an estimated false discovery rate of 10%.

RESULTS

The 13 participants adhered to the 2 dietary periods of 4 wk each without any declared difficulty. According to self-report and physician recommendation, participants' lifestyles were unchanged throughout the study. The 2 diets did not significantly modify kidney functions as evaluated by measurement of plasma creatinine and cystatin C (**Table 2**).

Effects of LC-CONV and LC-P-LGI diets on bioclinical variables

Dietary intake

The results of the 7-d dietary records are presented in Table 2. According to dietary evaluation, the participants appeared to fulfill the recommendations. Total energy intake decreased significantly during the 2 dietary periods to reach ~1200 kcal in the 2 dietary arms. The participants significantly increased their protein intake, an increase that was higher after the LC-P-LGI diet than after the LC-CONV diet, as expected. Fat intake decreased significantly after the 2 dietary periods but was lower after the LC-P-LGI arm than after the LC-CONV arm. No significant difference was detected between the 2 dietary arms for carbohydrate intake. Therefore, the 2 diets were both hypocaloric with low fat content that was compensated by more protein in the LC-P-LGI diet. The main difference detected between the 2 diets was related to the protein and the lipid contents. For carbohydrate consumption, the quality but not the quantity differed between the 2 dietary periods.

During the washout period, the dietitian recommended that the participants keep their body weight constant by increasing their caloric intake slightly. Nine participants succeeded in keeping their body weight constant, whereas 4 experienced moderately increased body weight despite the recommendations.

Adiposity variables

Both diets led to significant body weight and fat loss, with a slight trend but nonsignificant advantage for total fat mass with the LC-P-LGI diet (Δ changes: $P = 0.10$), as shown in Table 2. Whereas the 2 diets similarly decreased lower body fat mass, the LC-P-LGI, but not the LC-CONV, diet significantly reduced trunk fat mass. Changes between the 2 dietary periods (−0.808 for LC-P-LGI compared with −0.125 kg for LC-CONV) showed a trend in favor of the LC-P-LGI ($P = 0.08$). Waist and hip circumferences decreased significantly in both diet arms. The LC-P-LGI diet tended to reduce waist circumference more ($P = 0.07$ for Δ changes between the 2 diets), whereas LC-CONV reduced hip circumference more ($P < 0.03$). There were no differences between android and gynoid fat mass between or during the 2 diets. A slight but nonsignificant sex difference was found in the distribution of gynoid and android fat mass. The 2 diets efficiently reduced adipocyte diameter, with a greater and significant reduction after the LC-P-LGI diet compared with the LC-CONV diet ($P < 0.048$).

Plasma glucose and lipid homeostasis

A significant decrease in fasting glucose was observed only after the LC-P-LGI diet. This decrease tended to be greater ($P = 0.07$) than that with the LC-CONV diet. Plasma insulin decreased with the 2 diets: the decrease with the LC-CONV diet tended to be higher than that with the LC-P-LGI diet ($P = 0.05$). The LC-CONV diet had more effect on the Δ change of HOMA-IR and HOMA-S %, whereas the LC-P-LGI diet affected the Δ change of HOMA-B % more, suggesting a trend for a better improvement of β cell function ($P = 0.09$).

Postprandial plasma glucose improved more with the LC-P-LGI diet than with the LC-CONV diet (data not shown).

No major difference was seen between the 2 dietary arms for plasma lipids. Compared with LC-CONV, a slight improvement in ΔLDL-cholesterol after the LC-P-LGI diet only was observed ($P = 0.057$).

Adipokines and inflammatory and cardiovascular risk factors

There were no significant differences during or between the 2 diets for adiponectin, IL-6, TNF-α, MIP-1A, MIP-1B, G-CSF, and eotaxin (Table 2). Plasma leptin decreased after both diets, with a trend toward a greater effect of the LC-P-LGI diet ($\Delta P = 0.10$).

The LC-P-LGI regimen reduced concentrations of PAI-1 and VEGF. hs-CRP decreased only after the LC-P-LGI diet, but no significant difference could be detected when the Δ changes between the 2 diets were compared. VEGF and PAI-1 decreased only after the LC-P-LGI diet, but there was a significant effect between the 2 diets. Another inflammatory marker (IP-10) increased during the LC-CONV diet, with no change or a tendency to decrease after the LC-P-LGI diet. A comparison of the 2 diets identified an improvement in IP-10 for the LC-P-LGI diet.

PDGF Δ change between the 2 dietary periods was greater after the LC-P-LGI diet than after the LC-CONV diet ($P = 0.02$). With regard to other risk factors, the 2 diets decreased the diastolic blood pressure, whereas the LC-CONV, but not the LC-P-LGI, diet decreased systolic blood pressure, but no significant difference could be detected when the Δ changes between the 2 diets were compared.

Global effect of the entire dietary intervention (16 wk) on bioclinical variables: associations with adipocyte diameters

We examined the global impact of this sequential interventional of two 4-wk energy-restricted diets separated by an 8-wk stabilization period (or washout period) (**Table 3**). This 16-wk intervention was associated with a significant loss of body weight and waist and hip circumferences and a mean 3.5-kg total fat mass loss. There was a significant reduction in adipocyte diameter (>20% reduction in micrometers, $P < 0.001$). In agreement with the reduction in body fat mass and adipocyte diameter, leptin concentrations decreased significantly. Fasting ghrelin increased. The systolic and diastolic blood pressures were ameliorated significantly.

TABLE 2
Clinical variables before and after 4 wk of each diet[1]

	LC-CONV			LC-P-LGI				
	Baseline	4 wk	*P*	Baseline	4 wk	*P*		Diet effect,[2] *P*
Dietary control								
Energy (kcal/d)	1877.77 ± 185.97	1283 ± 94.55	0.002	1630.4 ± 87.22	1199.08 ± 70.7	0.003	*	0.17
Carbohydrates (%)	44.77 ± 1.83	43.77 ± 2.05	0.34	44.6 ± 2.43	40.42 ± 1.45	0.03		0.11
Protein (%)	17.08 ± 0.98	21.46 ± 0.85	<0.001	18.7 ± 0.92	33.17 ± 1.66	<0.001	*	<0.001
Lipid (%)	38 ± 1.63	32.77 ± 1.86	0.04	35.9 ± 3.22	26.5 ± 1.68	0.01	*	0.03
Anthropometric variables								
Body weight (kg)	89.82 ± 3.66	87.08 ± 3.5	<0.001	90.4 ± 3.38	86.84 ± 3.37	<0.001	*	0.14
Waist circumference (cm)	107 ± 3.21	104.38 ± 3.08	<0.001	108.31 ± 3.67	103.54 ± 3.35	0.001	*	0.07
Hip circumference (cm)	107.92 ± 2.11	105.62 ± 2.05	<0.001	106.85 ± 2.28	105.92 ± 2.23	0.023	*	0.03
Blood pressure								
Systolic (mm Hg)	124.38 ± 3.22	116.69 ± 1.93	0.002	121.77 ± 3.02	117.62 ± 2.89	0.13		0.16
Diastolic (mm Hg)	77.23 ± 3.55	65.54 ± 1.85	0.002	75 ± 3.56	67.62 ± 2.19	0.02	*	0.22
Fat and fat-free mass								
Fat mass (kg)	28.25 ± 2.19	27.15 ± 2.28	0.009	28.72 ± 2.64	27.02 ± 2.58	<0.001	*	0.10
Fat mass (%)	31.64 ± 1.95	31.32 ± 2	0.199	31.97 ± 2.3	31.17 ± 2.4	0.101	*	0.26
Fat-free mass (kg)	57.85 ± 2.65	56.11 ± 2.45	<0.001	57.93 ± 2.24	55.84 ± 2.43	0.001	*	0.29
Fat-free mass (%)	65.12 ± 1.84	65.41 ± 1.91	0.23	64.88 ± 2.29	65.32 ± 2.31	0.172		0.39
Trunk fat mass (kg)	14.46 ± 1.39	14.33 ± 1.48	0.355	15.47 ± 1.53	14.66 ± 1.41	0.017	*	0.08
Lower body fat mass (kg)	10.60 ± 0.81	9.99 ± 0.74	0.003	10.87 ± 0.99	10.12 ± 1.08	0.005		0.32
Adipocyte diameter (μm)	102.12 ± 2.71	91.74 ± 2.61	0.003	109.94 ± 3.19	92.26 ± 4.27	<0.001	*	0.048
Glucose homeostasis								
Fasting plasma glucose (mmol/L)	4.73 ± 0.2	4.79 ± 0.24	0.37	5.13 ± 0.19	4.8 ± 0.23	0.033	*	0.07
Fasting plasma insulin (pmol/L)	8.17 ± 1.09	5.74 ± 0.93	<0.001	8.33 ± 1.52	6.75 ± 1.1	0.029	*	0.05
C-peptide (ng/mL)	0.509 ± 0.09	0.379 ± 0.05	0.09	0.524 ± 0.07	0.398 ± 0.05	0.005	*	0.48
HOMA-IR	0.85 ± 0.1	0.63 ± 0.08	0.005	0.81 ± 0.19	0.78 ± 0.13	0.341		0.03
HOMA-S (%)	144.45 ± 23.32	183.59 ± 20.71	0.24	160.68 ± 16.3	158.58 ± 19.14	0.440		0.04
HOMA-B (%)	92.93 ± 9.45	81.61 ± 10.87	0.17	75.05 ± 4.38	90.49 ± 8.37	0.047		0.09
Plasma lipid homeostasis								
Triacylglycerol (mmol/L)	1.75 ± 0.25	1.31 ± 0.16	0.011	1.51 ± 0.26	1.26 ± 0.16	0.063		0.18
Total cholesterol (mmol/L)	5.66 ± 0.33	5.24 ± 0.34	0.012	5.46 ± 0.37	4.68 ± 0.31	0.001	*	0.09
HDL cholesterol (mmol/L)	1.25 ± 0.09	1.19 ± 0.07	0.11	1.31 ± 0.09	1.2 ± 0.07	0.021	*	0.15
LDL cholestrol (mmol/L)	3.54 ± 0.29	3.43 ± 0.3	0.26	3.4 ± 0.31	2.89 ± 0.26	0.012		0.057
Atherogenic index[3]	0.092 ± 0.1	0.017 ± 0.06	0.10	0.007 ± 0.09	−0.007 ± 0.07	0.41		0.21
Adipokines and risk factors								
Leptin (ng/mL)	25.28 ± 2.38	17.98 ± 2.10	0.04	24.10 ± 1.77	12.48 ± 1.19	0.002	*	0.10
Ghrelin (pg/mL)	70.94 ± 4.7	75 ± 3.6	0.22	70.77 ± 4.5	78.36 ± 3.8	0.064		0.27
Adiponectin (μg/mL)	31.48 ± 4.5	29 ± 3.6	0.18	31.19 ± 4.5	32.13 ± 4.4	0.387		0.22
hs-CRP (mg/mL)	2.97 ± 0.74	3.4 ± 1.06	0.35	2.82 ± 0.61	2.36 ± 0.56	0.028	*	0.23
PAI-1 (ng/mL)	27.7 ± 2.6	28.87 ± 3.6	0.38	33.26 ± 2.6	23.99 ± 3	0.046	*	0.019
IL-6 (μg/mL)	3.22 ± 0.4	3.35 ± 0.42	0.41	2.91 ± 0.46	3.51 ± 0.36	0.18		0.25
IP-10 (μg/mL)	0.407 ± 0.05	0.547 ± 0.1	0.02	0.415 ± 0.06	0.354 ± 0.05	0.08		0.01
TNF-α (pg/mL)	2.84 ± 0.3	2.81 ± 0.21	0.45	3.24 ± 0.31	3.3 ± 0.42	0.45		0.41
MIP-1A (pg/mL)	9.01 ± 0.49	8.90 ± 0.44	0.33	8.56 ± 0.35	9.32 ± 0.96	0.17		0.14
MIP-1B (pg/mL)	51.61 ± 4.4	57.91 ± 5.54	0.058	46.48 ± 3.55	46.88 ± 3.08	0.45		0.12
PDGF (pg/mL)	65.16 ± 7.43	60.22 ± 6.56	0.26	74.78 ± 13.04	103.66 ± 18.07	0.056		0.020
G-CSF (pg/mL)	23.91 ± 2.77	27.77 ± 7.35	0.25	23.15 ± 4.3	27.79 ± 7.7	0.17		0.49
IL-1RA (pg/mL)	83.6 ± 8.1	92.7 ± 16.9	0.11	76.0 ± 12.1	101.49 ± 26.6	0.21		0.38
IFN-γ (pg/mL)	275.54 ± 18.6	289.3 ± 23.9	0.45	268.6 ± 17.4	317.1 ± 23.5	0.35		0.22
Eotaxin (pg/mL)	55.5 ± 6.8	55.12 ± 5.4	0.47	49.0 ± 6.3	49.9 ± 4.8	0.45		0.43
VEGF (pg/mL)	34.99 ± 6.2	41.55 ± 8.46	0.21	56.35 ± 10.8	38.09 ± 6.89	0.02	*	0.032
Renal function								
Creatinine (μmol/L)	73.43 ± 2.8	78.59 ± 2.6	0.09	79.61 ± 4.4	76.88 ± 3.1	0.27		0.12
Cystatin C (mg/L)	1.17 ± 0.06	1.13 ± 0.04	0.20	1.13 ± 0.04	1.12 ± 0.04	0.47		0.34

[1] Values are means ± SEMs unless otherwise indicated. *n* = 13 subjects. Comparisons between baseline and 4-wk results for each type of diet were obtained by paired Student's t test. *Significant overall comparison between the 4 repeated outcomes by using multivariate analysis of repeated measurements. G-CSF, granulocyte colony-stimulating factor; HOMA-B, B cell function; HOMA-S, insulin sensitivity; hs-CRP, high-sensitivity C-reactive protein; IFN-γ, interferon γ; IL-1RA, IL-1 receptor antagonist; IP-10, interferon-γ inducible protein 10; LC-CONV, low-calorie conventional diet; LC-P-LGI, low-calorie, high-protein, low–glycemic index diet; MIP-1A, macrophage inflammatory protein 1A; MIP-1B, macrophage inflammatory protein 1B; PAI-1, plasminogen activator inhibitor protein-1; PDGF, platelet-derived growth factor; VEGF, vascular endothelial growth factor.

[2] Diet effect: the difference between the 2 diets assessed by comparing the Δ changes during each dietary period, which are equal to the diet × time interaction.

[3] Atherogenic index: log(triacylglycerols/HDL cholesterol).

Fasting plasma glucose and plasma insulin were significantly lowered, but no significant changes in insulin resistance (HOMA-IR) could be observed. No change in plasma adiponectin or major modifications in lipid variables were seen.

At the end of the entire dietary intervention, inflammatory factors such as hs-CRP, PAI-1, TNF-α, MIP-A, MIP-1B, G-CSF, IFN-γ, and eotaxin did not differ from basal values. We made a similar observation for PDGF. The antiangiogenic protein VEGF tended to decrease ($P = 0.07$). The cytokine IL-6 increased significantly ($P < 0.03$) at the end of the study, whereas the cytokines IP-10 ($P < 0.04$) and IL-1 ($P < 0.03$) receptor antagonist decreased significantly.

Of interest, we found significant correlations between the adipocyte diameters measured at each time point and several adiposity markers, adipokines, and metabolic risk variables after adjustment for percentage fat mass in a multivariate model, as shown in Supplementary Table 4 under "Supplemental data" in the online issue. Adiposity markers (body weight, fat mass, trunk fat mass, waist and hip circumferences, and plasma leptin), plasma glucose, plasma insulin, HOMA-IR, and systolic blood pressure correlated positively with adipocyte diameter, which changed drastically during the 16-wk intervention. Of importance, total energy intake and carbohydrate, protein, and lipid intakes also correlated positively with adipocyte size.

As also shown in Supplementary Table 4 under "Supplemental data" in the online issue, plasma lipids (triglycerides and total cholesterol) and the atherogenic index [log (triacylglycerols/HDL cholesterol)] were correlated to adipocyte diameter. In contrast, all of the measured inflammatory markers and adipokines, except for leptin and adiponectin, did not correlate significantly with adipocyte diameter. When considering each of the 2 diets separately, adipocyte size was correlated positively with plasma glucose and HOMA-IR and showed a trend with plasma PAI-1 changes during the LC-P-LGI diet but not during the LC-CONV diet (Supplementary Table 4 under "Supplemental data" in the online issue). During the LC-CONV diet, but not during the LC-P-LGI diet, diameter was correlated with triacylglycerol and the atherogenic index. Trunk fat mass, plasma insulin, and C-peptides were correlated positively with the adipocyte diameter, whereas adiponectin was correlated negatively during the 2 diets.

Correlations between Δ changes in adipocyte diameter and Δ changes in the clinical variables adjusted by percentage fat mass (**Table 4**) focused again on some important parameters. Taken together, Δ changes in adipocyte diameter remained correlated with Δ changes in some adiposity markers (BMI, total and trunk fat mass, and waist circumference) as well as Δ fasting plasma glucose between the start and the end of the program (16 wk). Of interest, during the LC-P-LGI diet, total fat mass correlation remained, whereas that with trunk fat mass and atherogenic index changes showed trends. Strong correlations were observed with plasma triacylglycerol, adiponectin, and IP-10. The main correlation presented in the LC-CONV diet was that with hip circumference and C-peptide.

Effect of the dietary intervention on gene expression profiles in subcutaneous adipose tissue: association with adipocyte diameter

First, a comparison of the gene expression profiles between the 2 energy-restricted diets showed no significant differences, indicating that there was no major macronutrient difference effect on whole-gene expression changes. Similarly, we found no period effect on modulated gene expression [ie, no significant differences in gene expression profiles were observed between a diet consumed either during the first period of the program (days 0–30) and during the second period (days 90–120)]. We then analyzed the kinetics of the adipose tissue transcriptomic signature during the entire dietary weight-loss intervention. This analysis included all time points for the 2 repeated dietary-restriction periods separated by a stabilization period (ie, day 0, day 5, day 30, day 90, day 95, and day 120). In addition, because the major change seen with this dietary intervention was related to modification of adipocyte diameter, we examined the association between subcutaneous gene expression changes and adipocyte diameter variation. This analysis was performed in the 10 participants for whom all paired data at all time points were available. The kinetic evolution of genes during the entire dietary intervention showed significant changes in the expression of 279 genes: 138 were upregulated, whereas 141 genes were downregulated (Supplementary Table 6 under "Supplemental data" in the online issue). As shown in **Figure 1**, genes with expression changes during the dietary weight-loss intervention were grouped with the following GO biological process annotations: upregulated genes were shown to be involved in functions such as "cell adhesion," "negative regulation of cell proliferation," "regulation of growth and motility," "cytoskeleton organization," and "defense response"; downregulated genes were shown to be involved in functions related to "oxidation reduction and oxidative stress," "protein transport," "response to hormone stimulus," "cell migration and regulation of cell growth," and "small GTPase-mediated signal transduction." Four functional modules (depicted with different node shapes) were identified by the FunNet tool, as shown in Supplementary Figure 2 and Supplementary Table 7 under "Supplemental data" in the online issue.

As shown in **Table 5**, among the genes that were modulated significantly during the entire dietary intervention and grouped in the above-mentioned functions, 78 genes correlated with adipocyte diameter, 40 genes were upregulated during the dietary intervention and were correlated negatively with adipocyte size (29% of overexpressed genes), and 38 genes (27% of downregulated genes) showed the opposite behavior (**Figure 2**). As shown in **Figure 3**, the 78 genes were grouped together in different modules in the coexpression network, which was composed of all of the genes that were significantly modulated during the entire energy-restricted dietary intervention. They were more particularly clustered in the functional categories as shown in Supplementary Figure 2 and Supplementary Table 4 (under "Supplemental data" in the online issue. The list (Table 5) included genes implicated in the regulation of cell proliferation (*GAL*, *GPC3*, *CUL1*, *IGFBP3*, *FTH1*, *FTHL11*, *CREG1*, *ZFP36L2*, *SERPINDF1*), regulation of growth (*CRIM1*, *CREG1*, *GPC3*, *IGFBP3*), cell adhesion (*STAT5A*, *TYRO3*, *AHI1*, *FNDC4*), cell migration (*NCK1*, *CCL22*, *RRAS2*, *MMP9*, *NR2F1*), negative regulation of cell motility (*IGFBP3*), cell components (*FAM3A*), apoptosis (*BAG3*, *CUL1*, *IGFBP3*, *MMP9*, *SGPP1*, *GAL*, *PDCL3*, *RNF144B*, *CSTP*, *STATS5A*, *GPC3*), oxidation reduction processes (*KDM1A*, *SQLE*, *SRXN1*, *GATM*, *ALDH18A1*), response to oxidative stress (*GATM*, *SRXN1*), negative regulation of inflammatory responses or macrophage

TABLE 3
Clinical variables before and at the end of the total 16-wk dietary intervention[1]

	Start of study	End of study	Change (*Δ*)	*P*
Dietary control				
Energy (kcal/d)	1820 ± 199	1287 ± 69	−532 ± 637	0.004
Carbohydrate (%)	44.46 ± 1.65	42.67 ± 1.60	−1.76 ± 2.42	0.24
Protein (%)	16.33 ± 1.02	26.08 ± 1.88	9.10 ± 4.42	0.003
Lipid (%)	39.11 ± 1.93	33.42 ± 1.53	−5.10 ± 2.68	0.03
Anthropometric variables				
Body weight (kg)	92.05 ± 7.67	86.05 ± 7.17	−6.01 ± 1.3	<0.001
Waist circumference (cm)	110.84 ± 3.49	102.15 ± 3.18	−8.69 ± 2.07	<0.001
Hip circumference (cm)	108.69 ± 2.32	104.92 ± 2.07	−3.77 ± 1.12	0.002
Blood pressure				
Systolic (mm Hg)	124.54 ± 3.09	114.62 ± 1.85	−10.46 ± 2.8	0.002
Diastolic (mm Hg)	84.62 ± 4.34	66.31 ± 1.91	−15.31 ± 3.46	0.001
Body composition				
Fat mass (kg)	29.74 ± 2.43	26.22 ± 2.45	−3.53 ± 1.11	0.003
Fat mass (%)	32.14 ± 2.03	30.49 ± 2.21	−1.65 ± 0.86	0.030
Fat-free mass (kg)	58.50 ± 2.27	56.00 ± 2.47	−2.50 ± 0.54	<0.001
Fat-free mass (%)	64.45 ± 1.96	65.99 ± 2.14	1.53 ± 0.93	0.056
Trunk fat mass (kg)	15.27 ± 1.37	13.33 ± 1.50	−1.93 ± 0.69	0.007
Lower body fat mass (kg)	11.02 ± 0.93	9.16 ± 0.81	−1.86 ± 0.59	0.003
Adipocyte diameter (*μ*m)	108.19 ± 9.09	84.54 ± 7.04	−23.66 ± 3.74	<0.001
Glucose homeostasis				
Fasting plasma glucose (mmol/L)	5.15 ± 0.23	4.39 ± 0.23	−0.76 ± 0.25	0.004
Fasting plasma insulin (pmol/L)	8.70 ± 0.14	5.87 ± 0.97	−2.83 ± 1.57	0.04
C-peptide (ng/mL)	0.513 ± 0.080	0.386 ± 0.05	−0.126 ± 0.08	0.07
HOMA-IR	0.87 ± 0.19	0.67 ± 0.09	−0.19 ± 0.18	0.16
HOMA-S (%)	135.36 ± 17.77	159.17 ± 23.62	15.19 ± 5.83	0.23
HOMA-B (%)	75.78 ± 8.29	75.95 ± 11.58	2.70 ± 1.59	0.24
Plasma lipid homeostasis				
Triacylglycerol (mmol/L)	1.60 ± 0.25	1.32 ± 0.16	−0.28 ± 0.22	0.11
Total cholesterol (mmol/L)	5.55 ± 0.43	5.14 ± 0.33	−0.41 ± 0.29	0.09
HDL cholesterol (mmol/L)	1.25 ± 0.10	1.21 ± 0.07	−0.04 ± 0.06	0.14
LDL cholestrol (mmol/L)	3.48 ± 0.37	3.3 ± 0.31	−0.19 ± 0.3	0.45
Atherogenic index	0.06 ± 0.1	0.01 ± 0.06	−0.05 ± 0.07	0.33
Adipokines and risk factors				
Leptin (ng/mL)	26.94 ± 2.0	17.40 ± 1.23	−5.81 ± 2.2	0.01
Ghrelin (pg/mL)	68.36 ± 4.6	77.56 ± 3.9	8.26 ± 4.3	0.04
Adiponectin (*μ*g/mL)	13.66 ± 0.73	12.78 ± 0.78	−1.86 ± 0.70	0.17
hs-CRP (mg/L)	2.51 ± 0.59	2.76 ± 0.66	0.25 ± 0.44	0.28
PAI-1 (ng/mL)	32.05 ± 3.5	30.99 ± 4.1	−1.06 ± 4.8	0.41
IL-6 (*μ*g/mL)	2.63 ± 0.48	3.58 ± 0.43	1.22 ± 0.59	0.03
IP-10 (*μ*g/mL)	456.87 ± 62.39	372.54 ± 45.09	−84.33 ± 46.46	0.04
TNF-*α* (pg/mL)	2.73 ± 0.29	3.11 ± 0.39	0.38 ± 0.42	0.42
MIP-1A (pg/mL)	8.85 ± 0.53	9.21 ± 1.27	1.86 ± 1.24	0.27
MIP-1B (pg/mL))	48.71 ± 1.4	49.75 ± 0.4	7.04 ± 3.9	0.47
PDGF (pg/mL)	78.5 ± 13.07	69.15 ± 8.01	−9.35 ± 16.11	0.27
G-CSF (pg/mL)	23.91 ± 2.76	23.98 ± 7.81	0.06 ± 6.17	0.49
IL-1RA (pg/mL)	77.8 ± 9.2	58.6 ± 7.8	−19.16 ± 9.2	0.03
IFN-*γ* (pg/mL)	296.6 ± 15.94	304.38 ± 19.96	7.76 ± 24.04	0.37
Eotaxin (pg/mL)	41.64 ± 6.44	43.89 ± 8.81	0.63 ± 7.33	0.46
VEGF (pg/mL)	58.02 ± 2.53	42.91 ± 9.7	−12.79 ± 9.37	0.07

[1] All values are means ± SEMs. *n* = 13 subjects. Statistical analysis was performed by using Student's *t* test for paired data. G-CSF, granulocyte colony-stimulating factor; HOMA-B, B cell function; HOMA-S, insulin sensitivity; hs-CRP, high-sensitivity C-reactive protein; IFN-*γ* , interferon *γ*; IL-1RA, IL-1 receptor antagonist; IP-10, interferon-*γ* inducible protein 10; MIP-1A, macrophage inflammatory protein 1A; MIP-1B, macrophage inflammatory protein 1B; PAI-1, plasminogen activator inhibitor protein-1; PDGF, platelet-derived growth factor; VEGF, vascular endothelial growth factor; *Δ*; data at the end of the entire dietary intervention of 16 wk minus data at study baseline.

differentiation (*MMP9*, *SERPINF1*, *GAL*, *ABCA1*, *CCL22*), autophagy (*WIPI1*), endocytosis (*GPC3*), metabolic processes (*CETP*, *SQLE*, *ABCA1*, *MMP9*, *HDC*), defense response (*DCD*), protein transport (*ACAP1*, *TIMM16*, *RAB38*, *CHMP1B*), small GTPase activity (*TUBG2*, *RRAS2*, *RAB36*), and steroid metabolic processes (*GATM*, *ABCA1*).

TABLE 4

Correlations between Δ adipocyte changes and Δ changes in clinical variables adjusted by percentage fat mass during the 2 dietary periods and during the entire dietary intervention[1]

	During the entire time course		During the LC-P-LGI		During the LC-CONV	
	ρ	P value	ρ	P value	ρ	P value
Body weight (kg)	0.537	0.056	0.463	0.117	−0.073	0.826
BMI (kg/m^2)	0.734	0.001	0.33	0.295	−0.096	0.772
Waist circumference (cm)	0.635	0.014	0.432	0.151	−0.2	0.541
Hip circumference (cm)	0.014	0.966	−0.142	0.668	-0.786	<0.001
Fat mass (kg)	0.719	0.002	0.638	0.013	−0.241	0.456
Trunk fat mass (kg)	0.796	0.001	0.536	0.093	0.145	0.697
Fasting plasma glucose (mmol/L)	0.587	0.029	0.288	0.367	0.129	0.697
C-peptide (ng/mL)	0.387	0.267	−0.009	0.981	0.573	0.048
Triacylglycerol (mmol/L)	0.31	0.328	0.567	0.039	−0.065	0.846
Atherogenic index	0.138	0.675	0.526	0.063	0.073	0.826
Adiponectin (μg/mL)	0.481	0.099	0.694	0.004	0.349	0.264
IP-10 (μg/mL)	−0.365	0.24	−0.661	0.008	0.2	0.541

[1] $n = 13$. Only variables with significant P values, or trends, and relevant ρ values, in at least one of the studied conditions are presented. IP-10, interferon-γ inducible protein 10; LC-CONV, low-calorie conventional diet; LC-P-LGI, low-calorie, high-protein, low–glycemic index diet.

When these correlations were adjusted for fat mass (Table 5), some of the correlations disappeared, indicating their dependence on fat mass during the entire dietary intervention. These included the correlations with *SERPINF1* and some but not all of the genes included in the following functions: oxidation reduction process (*ALDH18A1*, *KMD1A*, *FTH1*, *FTHL11*), cell adhesion (*STAT5A*), negative regulation of cell proliferation (*FTH1*, *FTHL11*), cellular growth, and apoptosis.

Some of the correlations between adipocyte diameters and gene expression changes were more significant with the LC-P-LGI diet, as shown in Supplementary Table 5 under "Supplemental data" in the online issue. The associations with *SERPINF1* and *RRAS2* were dependent on body fat mass in the multivariate model.

DISCUSSION

LGI diets have been proven to be beneficial for weight loss (21) and for weight maintenance when associated with a modest increase in protein content (5). The consequences of such diets on adipose tissue biology are not well known, even if no major difference in macronutrient composition was seen in the exploration of adipose tissue in participants involved in weight-maintenance programs (22). In global agreement with these studies, we showed here by using a crossover design that an LC-CONV diet and an LC-P-LGI diet with soluble fiber were similarly effective in reducing weight in moderately obese participants. Subtle differences were seen only as trends toward more reduction in total and trunk fat mass and waist circumference with the LC-P-LGI diet and toward a higher reduction in hip circumference with the LC-CONV diet. A major phenotype that was observed over time in our study was the reduction in fat cell size in the 2 arms of the dietary intervention. Adipocyte diameter is an important cellular obesity phenotype (8) that has never been investigated in this context. Our study identified a greater reduction in adipocyte size after the LC-P-LGI diet than after the LC-CONV diet. This could be responsible in part for the decrease in trunk fat mass with the LC-P-LGI diet. Of note, the dynamic reduction in adipocyte diameter during the entire intervention as well as Δ variation were strongly associated with reducing trunk fat mass but not with lower body fat mass. The same association was found when correlating Δ differences during the entire intervention and as a trend during the LC-P-LGI diet. This association between abdominal fat mass and adipocyte diameter is similar to results in a cohort of normal-weight subjects (23), but not in a longitudinal approach in obese subjects as in the present study.

The relevance of adipocyte diameter as a phenotype in such a dietary intervention was further shown by the dynamic correlations between this cellular phenotype and the improvement in metabolic variables such as plasma glucose, insulin, HOMA-IR, and the atherogenic index. This is in agreement with results observed in normal-weight subjects (24) and not in a longitudinal approach. Better correlations with insulin-resistant surrogates independent of fat mass variations were found with the LC-P-LGI diet compared with the LC-CONV diet. Adiponectin, another insulin sensitivity marker, which did not show major changes in the 2 dietary arms or during the overall intervention, negatively correlated with adipocyte size kinetic variations. Correlations of Δ variations were more apparent in the LG-P-LGI diet. Of interest, these correlations were independent of fat mass changes. Weight-stable nonobese and obese individuals with increased adipocyte cell size for a similar amount of fat mass indeed have greater insulin resistance (25). Whereas adipocyte size is not the best predictor of metabolic disorders during obesity (24), our study likely extends the importance of individual adipocyte size variation as a marker associated with changes in insulin sensitivity and abdominal obesity in weight-loss programs, with a significant contribution shown by the LC-P-LGI diet.

The LC-P-LGI diet induced an improvement in fasting plasma glucose, which could not be detected after the LC-CONV diet. Energy-restricted diets, whether low-fat or low-carbohydrate and with or without LGI, have failed to ameliorate fasting plasma

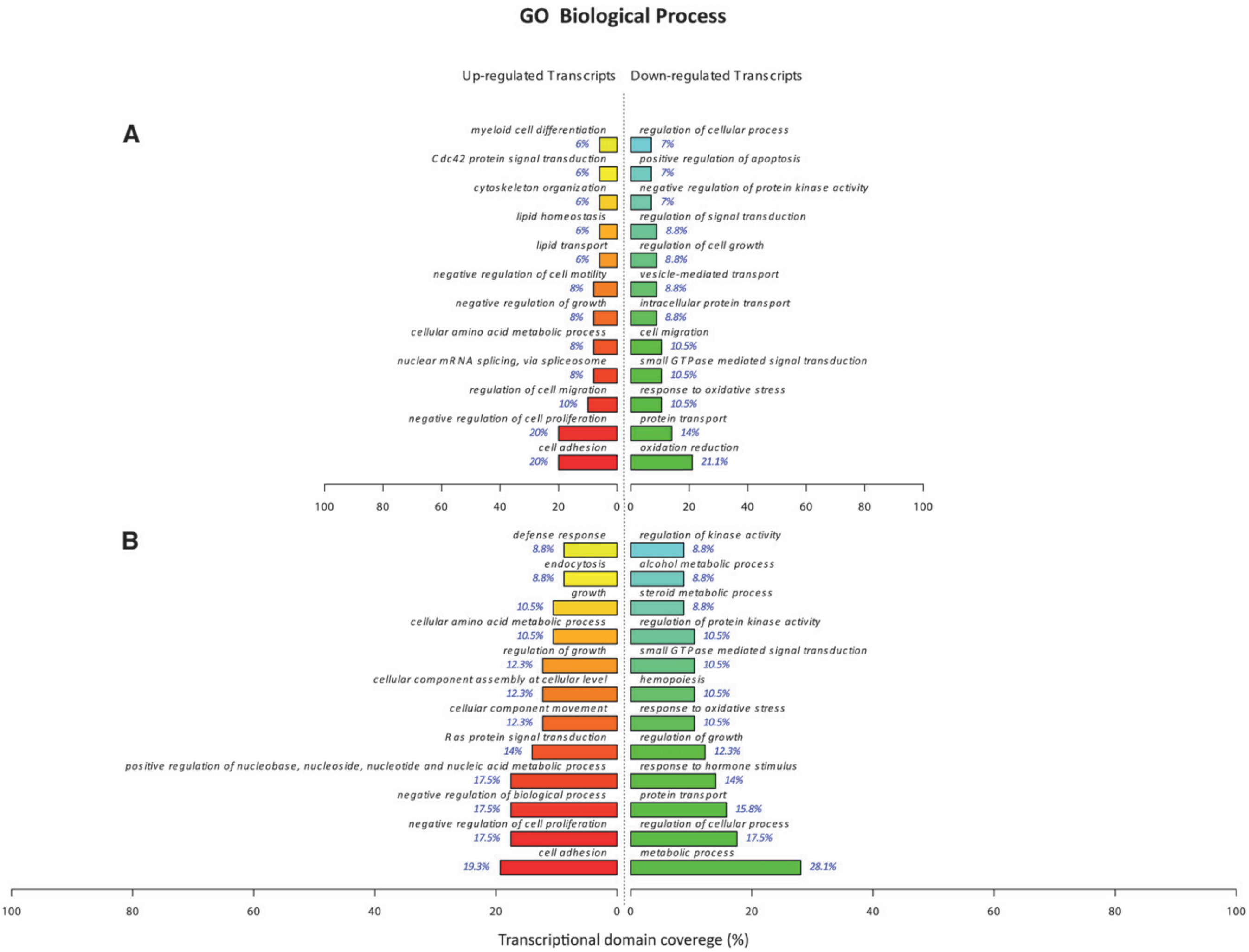

FIGURE 1. Functional annotation of the 2 lists of genes (ie, 138 up- and 141 downregulated) with expression discriminated by the energy-restricted dietary intervention in subcutaneous adipose tissue. Functional profiles show the transcriptomic signature of the energy-restriction modulated genes annotated by the GO biological process: A: level 5; B: level 7. GO, Gene Ontology.

glucose (26, 27) in obese healthy participants, in contrast to the amelioration of plasma glucose in diabetic individuals (28). One explanation of the improvement in plasma glucose in healthy participants in the present study could be that the LC-P-LGI was also enriched in protein, delaying further gastric emptying, and that the soluble fiber changed the viscosity properties. The fact that dynamic as well as *Δ* changes of adipocyte diameter positively correlated with plasma glucose strengthens the relation between adipocyte size and glucose metabolism, indicating an impact of plasma glucose concentrations in regulating adipocyte size during a weight-loss program. Imbalance in glucose-insulin homeostasis was found to be associated to enlarged abdominal adipocytes (29).

Of particular relevance is the fact that the LC-P-LGI diet was more effective than the LC-CONV diet in reducing some cardiovascular risk factors (30–32), such as hs-CRP, VEGF, and PAI-1. Several studies suggested that high hs-CRP precedes atheromatic events even in subjects without known cardiovascular risk (33). Therefore, any strategy to reduce hs-CRP, such as the LC-P-LGI diet in the present study, is of health benefit. As previously shown, VEGF decreased with marked weight loss and increased with weight gain (34). Several weight-loss programs involving energy-restricted diets improved plasma PAI-1 (35). VEGF and PAI-1 exert many local and systemic biological effects. They act as angiogenic factors (31) in the adipose tissue and contribute to the regulation of growth (36). Deficiency in plasminogen is associated with the reduction in fat accumulation and diminished differentiation of stromal cells (37). During dietary restriction in rodents, VEGF-A was found to be correlated with tissue weight and fat mass depots (38). It is a key mediator of the coupling of adipogenesis and angiogenesis, which is essential for adipocyte differentiation in obesity (39, 40). Adipose tissue is highly vascularized, indicating that remodeling of the vascularization takes place during its hypertrophy (39, 41). Recently, it has been shown that blockade of neovascularization with angiogenesis inhibitors results in weight reduction and adipose tissue loss (39). The question is open as to whether the decrease in VEGF affects changes in tissue vascularization and adipose differentiation capacity differentially during energy-restricted diets with different nutrients. Further reduction in abdominal mass in the LC-P-LGI diet might be responsible in part for greater decrease in cardiovascular risk factors. Many other factors independent of fat mass could be implicated, such as fasting plasma glucose concentrations (42).

TABLE 5

Genes modulated significantly during the entire dietary intervention and correlated to changes in adipocyte diameter[1]

Symbol	Name	GeneID	*r*	*P* value	Functions
Upregulated genes					
IGFBP3	Insulin-like growth factor binding protein 3	3486	−0.51	<0.001	Negative regulation of cell proliferation, negative regulation of smooth muscle cell migration, positive regulation of apoptosis
MRPS2	Mitochondrial ribosomal protein S2	51116	−0.52	<0.001	Cellular component, small ribosomal subunit
C14orf139	Chromosome 14 open reading frame 139	79686	−0.51	<0.001	Unknown
RPL35P2	Ribosomal protein L35 pseudogene 2	646766	−0.46	<0.001	Unknown
CUL1	Cullin 1	8454	−0.45	<0.001	Negative regulation of cell proliferation
AHI1	Abelson helper integration site 1	54806	−0.44	<0.001	Cellular component, cytoskeleton, adherens junction
NEK1	NIMA (never in mitosis gene a)–related kinase 1	4750	−0.42	<0.001	Protein kinase activity, cell cycle, cell division, transferase activity
TIMM16	Mitochondria-associated protein	51025	−0.40	<0.001	Protein transport
LSM2	LSM2 homolog, U6 small nuclear RNA associated	57819	−0.40	<0.001	Nuclear mRNA splicing, via spliceosome
SNRPA	Small nuclear ribonucleoprotein polypeptide A	6626	−0.39	<0.001	Nuclear mRNA splicing, via spliceosome
C5orf15	Chromosome 5 open reading frame 15	56951	−0.37	<0.001	Cellular component, integral to membrane
MUM1[2]	Melanoma-associated antigen (mutated) 1	84939	−0.37	<0.001	Protein binding, rhythmic process
TEF[2]	Thyrotrophic embryonic factor	7008	−0.37	<0.001	Rhythmic process
FNDC4	Fibronectin type III domain containing 4	64838	−0.36	<0.001	Cellular component
SERPINF1[2]	Serpin peptidase inhibitor, clade F1 (α-2 antiplasmin, pigment epithelium derived factor)	5176	−0.35	<0.001	Negative regulation of angiogenesis, negative regulation of inflammatory response
CETP	Cholesteryl ester transfer protein, plasma	1071	−0.35	<0.001	Regulation of cholesterol efflux, negative regulation of macrophage derived foam cell differentiation
ABCA1	ATP-binding cassette, subfamily A member 1	19	−0.34	<0.001	Steroid metabolic process, phagocytosis
RPL23AP45	Ribosomal protein L23a pseudogene 45	729764	−0.34	<0.001	Unknown
HDC	Histidine decarboxylase	3067	−0.33	<0.001	Cellular amino acid metabolic process
FAM3A	Family with sequence similarity 3 A	60343	−0.32	<0.001	Cellular component
DCD	Dermcidin	117159	−0.33	<0.001	Defense response to bacterium
H1FX	H1 histone family, member X	8971	−0.33	<0.001	Cellular component, DNA binding
C9orf123	Chromosome 9 open reading frame 123	90871	−0.33	<0.001	Cellular component
ZMYM1[2]	Zinc finger, MYM-type 1	79830	−0.33	<0.001	Nucleic acid binding, metal ion binding
STAT5A[2]	Signal transducer and activator of transcription 5A	6776	−0.33	<0.001	Regulation of cell adhesion, regulation of steroid metabolic process
NRIP1[2]	Nuclear receptor interacting protein 1	8204	−0.32	<0.001	Lipid storage|protein binding
CEBPZ	CCAAT/enhancer binding protein (C/EBP), zeta	10153	−0.32	<0.001	Cellular component, transcription from RNA polymerase
MUCL1	Mucin-like 1	118430	−0.31	<0.001	Extracellular region
ALDH18A1[2]	Aldehyde dehydrogenase 18 family A1	5832	−0.31	<0.001	Kinase activity|oxidation-reduction process
GPC3	Glypican 3	2719	−0.31	<0.001	Negative regulation of cell proliferation, positive regulation of endocytosis, negative regulation of growth
RFTN1	Raftlin, lipid raft linker 1	23180	−0.31	<0.001	Cell component
ACAP1[2]	ArfGAP with coiled-coil, ankyrin repeat and PH domains 1	9744	−0.30	<0.001	Protein transport
TYRO3	TYRO3 protein tyrosine kinase	7301	−0.30	<0.001	Cell adhesion
MGC24103	Hypothetical MGC24103	158295	−0.30	<0.001	Unknown
POLE4[2]	Polymerase (DNA-directed), epsilon 4 (p12 subunit)	56655	−0.29	<0.001	Transferase activity, cellular component, protein binding
KDM1A[2]	Lysine (K)-specific demethylase 1A	23028	−0.29	<0.001	FAD or FADH$_2$ binding, oxidation-reduction process

(Continued)

TABLE 5 (*Continued*)

Symbol	Name	GeneID	*r*	*P* value	Functions
Downregulated genes					
CSTB	Cystatin B	1476	0.60	<0.001	Regulation of apoptosis, cysteine-type endopeptidase inhibitor
SQLE	Squalene epoxidase	6713	0.60	<0.001	FAD or FADH$_2$ binding, cholesterol metabolic process, oxidation-reduction process
CCL22	Chemokine (C-C motif) ligand 22	6367	0.55	<0.001	Chemokine activity, cell migration, cell-cell signaling, immune response, inflammatory response
TUBG2	Tubulin, gamma 2	27175	0.56	<0.001	GTPase activity
ATP6V1A	ATPase, H+ transporting V1 subunit A	523	0.51	<0.001	ATP metabolic process
BAG3	BCL2-associated athanogene 3	9531	0.50	<0.001	Antiapoptosis
NR2F1	Nuclear receptor subfamily 2, group F1	7025	0.48	<0.001	Steroid hormone receptor activity
MMP9	Matrix metallopeptidase 9	4318	0.48	<0.001	Macrophage differentiation, metabolic process, positive regulation of apoptosis
RRAS2	Related RAS viral (r-ras) oncogene homolog 2	22800	0.46	0.001	GTPase activity, positive regulation of cell migration
UCHL1	Ubiquitin carboxyl-terminal esterase L1	7345	0.44	0.001	Negative regulation of MAP kinase activity
MSC[2]	Musculin (activated B cell factor 1)	9242	0.45	0.001	DNA binding
PDCL3	Phosducin-like 3	79031	0.43	0.002	Apoptosis
FTH1[2]	Ferritin, heavy polypeptide 1	2495	0.42	0.003	Negative regulation of cell proliferation, oxidation-reduction process
GATM	Glycine amidinotransferase	2628	0.41	0.003	Response to oxidative stress
FAM45A	Family with sequence similarity 45, member A	404636	0.37	0.009	Unknown
GAL	Galanin prepropeptide	51083	0.37	0.009	Inflammatory response, positive regulation of apoptosis
SLC31A2[2]	Solute carrier family 31 (copper transporters), member 2	1318	0.36	0.011	Copper ion transport
JAKMIP3[2]	Janus kinase and microtubule interacting protein 3	282973	0.36	0.012	Golgi apparatus, cellular component
RAB38	RAB38, member RAS oncogene family	23682	0.36	0.012	Protein transport, small GTPase mediated signal transduction
FTHL11[2]	Ferritin, heavy polypeptide-like 11	2503	0.35	0.014	Negative regulation of cell proliferation, oxidation-reduction process
CHMP1B	Chromatin modifying protein 1B	57132	0.35	0.014	Protein transport, cell division
PSMC4	Proteasome (prosome, macropain) 26S subunit, ATPase, 4	5704	0.34	0.016	Negative regulation of ubiquitin-protein ligase activity involved in mitotic cell cycle
CRIM1[2]	Cysteine-rich transmembrane BMP regulator 1	51232	0.35	0.015	Regulation of cell growth
CREG1[2]	Cellular repressor of E1A-stimulated genes 1	8804	0.34	0.017	Cell proliferation, regulation of growth
SGPP1	Sphingosine-1-phosphate phosphatase 1	81537	0.32	0.025	Apoptosis, sphingolipid metabolic process
RNF144B[2]	Ring finger protein 144B	255488	0.34	0.019	Apoptosis
WIPI1	WD repeat domain, phosphoinositide interacting 1	55062	0.33	0.023	Autophagy
CES8	Carboxylesterase 8 (putative)	283848	0.33	0.023	Carboxylesterase activity
NCK1[2]	NCK adaptor protein 1	4690	0.32	0.024	Cell migration, cytoskeletal adaptor activity
PQLC3	PQ loop repeat containing 3	130814	0.33	0.024	Cellular component
TNMD	Tenomodulin	64102	0.33	0.022	Angiogenesis inhibitor, cellular component
PSMD7	Proteasome (prosome, macropain) 26S non-ATPase, 7	5713	0.32	0.026	Negative regulation of mitotic cell cycle
RRAS2	Related RAS viral (r-ras) oncogene homolog 2	22800	0.32	0.028	GTPase activity, positive regulation of cell migration
LOC647349	(Sigma-adaptin 3a)	647349	0.31	0.030	Unknown
ZFP36L2	Zinc finger protein 36, C3H type-like 2	678	0.31	0.033	Cell proliferation
DDX21[2]	DEAD (Asp-Glu-Ala-Asp) box polypeptide 21	9188	0.31	0.033	Protein binding, RNA binding, helicase activity
SRXN1	Sulfiredoxin 1 homolog (*Saccharomyces cerevisiae*)	140809	0.31	0.033	Response to oxidative stress
YBX1P2	Y box binding protein 1 pseudogene 2	646531	0.31	0.034	Unknown
PDCL3	Phosducin-like 3	79031	0.30	0.037	Apoptosis

[1] ARFgap, ADP-ribosylation factor GTPase-activating protein; BCL2, B cell lymphoma 2; BMP, bone morphogenetic proteins; MAP kinase, mitogen-activated protein kinase; MYM, putative zinc-binding motif; NCK, non-catalytic region of tyrosin kinase adaptor protein 1; PQ, a novel family of membrane proteins; RAS subfamily, rat sarcoma, which is a protein subfamily of small GTPases; WD, proteins made up of highly conserved repeating units usually ending with Trp-Asp.

[2] Correlations with adipocyte diameter disappeared when adjusted for total percentage fat mass.

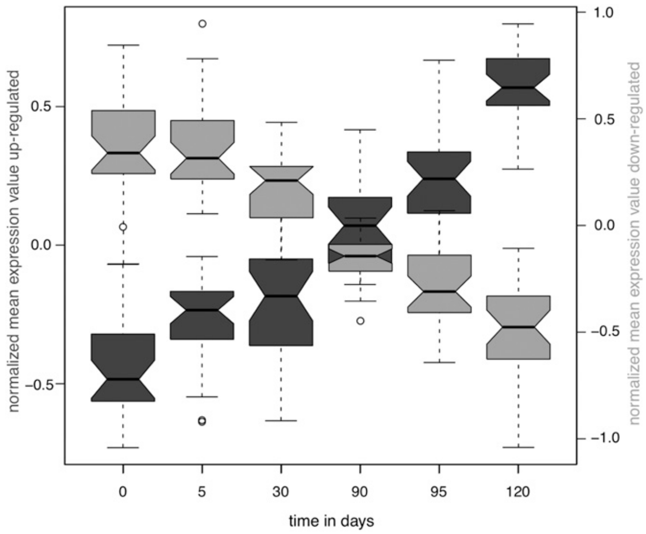

FIGURE 2. Boxplots representing gene expression profiles of the energy-restriction-modulated genes that correlated with adipocyte diameter. Black boxplots correspond to the genes that are upregulated, and gray boxplots correspond to those genes that are downregulated during the entire energy-restricted intervention. Open circles represent outliers.

Our study also raises the question of the association between adipose tissue remodeling and such mediators during different dietary interventions. The adipose tissue remodeling effect of the diets is shown by the pangenomic analysis of gene expression in subcutaneous adipose tissue. Globally, the dietary intervention with two different dietary periods was associated with changes in several genes, but no major differences were seen between the 2 dietary arms, which is in agreement with previous studies (6). However, the associations between changes in adipocyte size and a subset of genes implicated in the regulation of proliferation, adipogenesis, apoptosis, cell migration and adhesion, and angiogenesis are of utmost interest. During the entire dietary intervention, the positive associations between the decrease in adipocyte diameter and genes implicated in decreasing cell proliferation (*CUL1*, *IGFBP3*, *SERPINF1*, and *CREGI*) indicated a downregulation of adipose cell proliferation during the diet. Adipocyte diameter was correlated with antiapoptotic genes such as *BAG3* and *RNF144B* and negatively correlated with positive regulators of apoptosis such as *IGFBP3*. This observation and the proximity of functions related to "apoptosis," "proliferation," and "cell growth" may indicate the concomitant regulation of the apoptotic pathway and the regulation of adipocyte size. Many of the observed genes exert a variety of these functions, such as the *IGFBP3* gene, which was upregulated in the 2 dietary arms. It is also involved in angiogenesis but with contradictory effects that are tissue dependent (43, 44). *SERPINF1* also has a potent antiangiogenic activity (45). Broadly described, it represses tumor growth indirectly through the inhibition of angiogenesis and directly by inhibition of cell

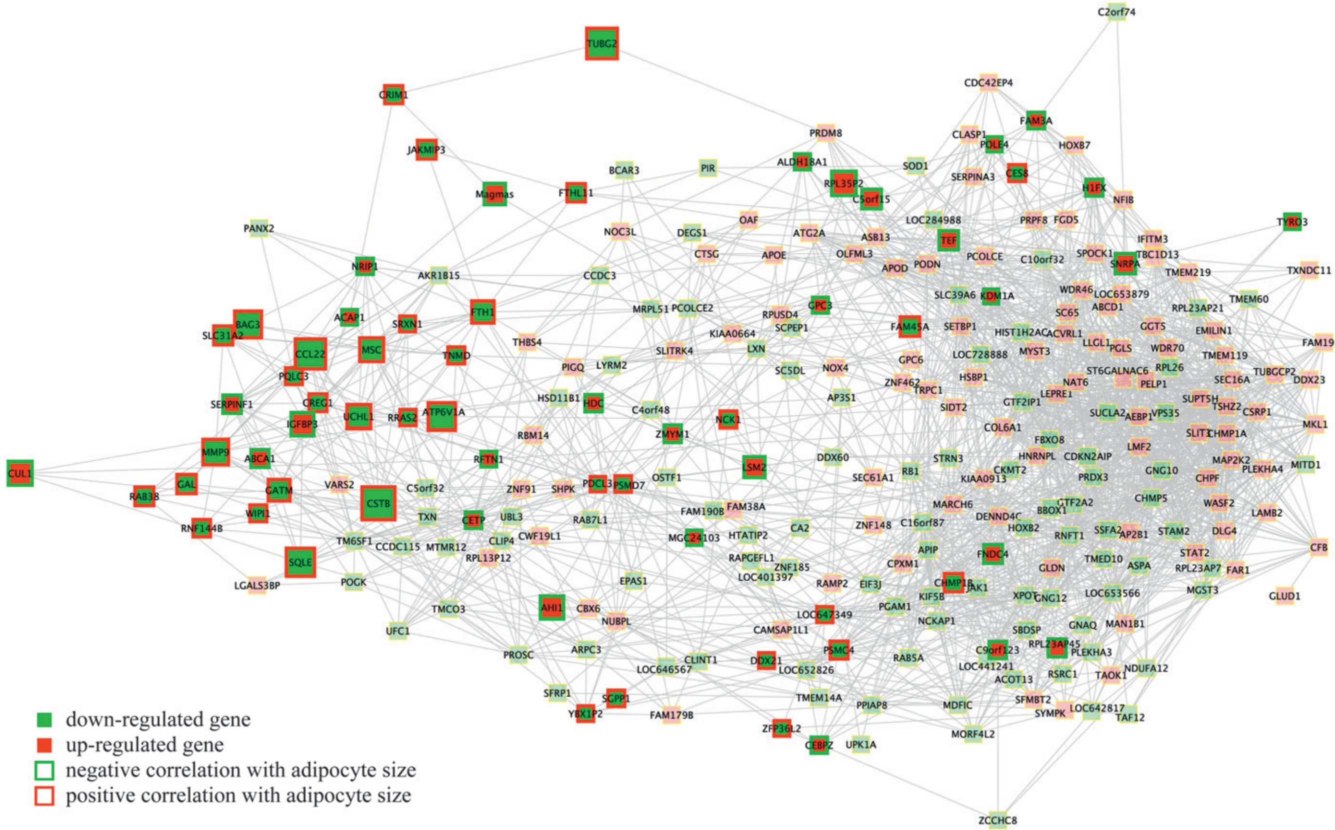

FIGURE 3. Coexpression network composed of 279 genes (ie, 138 up- and 141 downregulated), with expression discriminated by the energy-restricted diets. Genes (ie, represented by nodes in this network) are linked together if the coefficient correlation between their expression profiles is greater than that of a given threshold (hard threshold = 0.5). Nodes with strong red and green backgrounds identify the 78 genes that correlated significantly with adipocyte diameter. The size of the node is proportional to the correlation coefficient. The node frame color depicts the direction of the correlation (eg, red: positive correlation with adipocyte size; green: negative correlation with adipocyte size).

migration and induction of apoptosis (46). *SERPINF1* is highly expressed in human adipose tissue, and its plasma concentration is associated with central obesity (47). Of interest, the negative correlation between adipocyte size and *SERPINF1* was found only in the LC-P-LGI diet arm and was highly dependent on body fat mass. This finding may also indicate slight differences in adipogenic capacities and vascularization in the adipose tissue. These associations between diet-induced changes in adipocyte diameter and genes involved in apoptotic and angiogenic pathways underscore the need to better explore local remodeling changes in human adipose tissue and their association with systemic improvement of metabolic variables.

Whereas no correlations were found between systemic inflammation and adipocyte diameter, decreased adipocyte diameter was correlated with the inhibition of a subset of genes implicated in inflammation (positive correlation with *MMP9*, *CCL22*; negative correlation with *SERPINF1*). It is important to point out that all adipose tissue samples were obtained by needle biopsy, which poorly aspirates the fibrotic fraction of subcutaneous adipose tissue, resulting in an underrepresentation of the stroma-vascular fraction (48). Therefore, gene expression in adipose tissue in the present study reflects greater changes in adipocytes and to a lesser extent those in stromal-vascular fraction. Moreover, gene expression data may not reflect actual changes in protein expression and activity in the adipose tissue that should be further investigated.

Taken together, in the present study the comprehensive examination of genes associated with adipocyte size during the entire dietary weight-loss intervention highlighted a coordinated program involving molecular factors that inhibit adipogenesis, cell migration, adhesion, and angiogenesis but increase apoptosis. This longitudinal approach in a relatively small group of subjects paves the way for future in vitro and in vivo exploration of the relevance of these genes in determining cell morphology. It also opens avenues to explore in more depth the consequences of macronutrient consumption in modulating molecular factors involved in adipose tissue remodeling that could affect weight loss and maintenance. Note that the entire dietary intervention with 2 different, repeated, energy-restricted dietary periods separated by a stabilization period was of great health benefit for all of the subjects in terms of energy intake, adiposity, and most metabolic variables. This appears to be an easy and successful strategy in treatment of moderate obesity.

We are grateful to Sophie Gougis, registered dietitian, for dietary counseling to the patients and dietary data analysis. We thank Christine Baudoin, who was involved in patient recruitment, and Gregory Debrus, who contributed to patient follow-up. We also thank Soraya Fellahi for analyses of renal function markers. We acknowledge the group of Integragen, France: Francis Rousseau (director of Genomics), Maud Vanpeene (microarray analysis), and Stephanie Maillard (Fluidigm analysis). We are also grateful to Paul Kretchmer (San Francisco Edit) for the English revision of the manuscript.

The authors' responsibilities were as follows—SWR and KC: designed the research; SWR and FD: conducted the research; VP: prepared the adipose tissue and performed the microarray analysis; EP and VP: analyzed the biological interactions characterizing the transcriptomic signature; ML: analyzed and prepared glucose and insulin analyses; CR: performed and analyzed all cytokine analyses; SWR, LK, FK, and AC: analyzed data; SWR, KC, and FD: wrote the manuscript; RA and FM: designed the LC-P-LGI nutritional diet; FM: participated in the transcriptomic data analysis; and SWR: had primary responsibility for the final content. All authors read and approved the final manuscript. RA and FM are employees of CEPRODI-KOT Laboratory; they had no influence on the program, the study, or its conclusions. None of the other authors had a conflict of interest to declare.

REFERENCES

1. Astrup A, Rössner S. Lessons from obesity management programmes: greater initial weight loss improves long-term maintenance. Obes Rev 2000;1:17–9.
2. Weigle DS, Breen PA, Matthys CC, Callahan HS, Meeuws KE, Burden VR, Purnell JQ. A high-protein diet induces sustained reductions in appetite, ad libitum caloric intake, and body weight despite compensatory changes in diurnal plasma leptin and ghrelin concentrations. Am J Clin Nutr 2005;82:41–8.
3. Brand-Miller J, Holt S, Pawlak D, McMillan J. Glycemic index and obesity. Am J Clin Nutr 2002;76(1): 281S–5S.
4. Liu S, Willett W, Manson J, Hu F, Rosner B, Colditz G. Relation between changes in intakes of dietary fiber and grain products and changes in weight and development of obesity among middle-aged women. Am J Clin Nutr 2003;78:920–7.
5. Larsen TM, Dalskov SM, van Baak M, Jebb SA, Papadaki A, Pfeiffer AF, Martinez JA, Handjieva-Darlenska T, Kunesova M, Pihlsgard M, et al. Diets with high or low protein content and glycemic index for weight-loss maintenance. N Engl J Med 2010;363:2102–13.
6. Viguerie N, Poitou C, Cancello R, Stich V, Clement K, Langin D. Transcriptomics applied to obesity and caloric restriction. Biochimie 2005;87:117–23.
7. Clément K, Viguerie N, Poitou C, Carette C, Pelloux V, Curat CA, Sicard A, Rome S, Benis A, Zucker JD, et al. Weight loss regulates inflammation-related genes in white adipose tissue of obese subjects. FASEB J 2004;18:1657–69.
8. Hoffstedt J, Arner E, Wahrenberg H, Andersson DP, Qvisth V, Lofgren P, Ryden M, Thorne A, Wiren M, Palmer M, et al. Regional impact of adipose tissue morphology on the metabolic profile in morbid obesity. Diabetologia 2010;53:2496–503.
9. Pausova Z. From big fat cells to high blood pressure: a pathway to obesity-associated hypertension. Curr Opin Nephrol Hypertens 2006; 15:173–8.
10. Piatti PM, Monti LD, Baruffaldi L, Magni F, Paroni R, Fermo I, Costa S, Santambrogio G, Nasser R, Marchi M, et al. Effects of an acute increase in plasma triglyceride levels on glucose metabolism in man. Metabolism 1995;44:883–9.
11. Bouché C, Rizkalla S, Luo J, Vidal H, Veronese A, Pacher N, Fouquet C, Lang V, Slama G. Five week, low-glycemic idex diet decreases total fat mass and improves plasma lipid profile in moderately overweight non diabetic subjects. Diabetes Care 2002;25:822–8.
12. Matthews DR, Hosker J, Rudenski A, Naylor B, Treacher D, Turner RC. Homeostasis model assessment: insulin resistance and beta-cell function from fasting plasma glucose and insulin concentrations in man. Diabetologia 1985;28:412–9.
13. Rodbell M. Metabolism of isolated fat cells. I. Effects of hormones on glucose metabolism and lipolysis. J Biol Chem 1964;239:275–80.
14. Henegar C, Tordjman J, Achard V, Lacasa D, Cremer I, Guerre-Millo M, Poitou C, Basdevant A, Stich V, Viguerie N, et al. Adipose tissue transcriptomic signature highlights the pathological relevance of extracellular matrix in human obesity. Genome Biol 2008;9:R14.
15. Prifti E, Zucker JD, Clement K, Henegar C. FunNet: an integrative tool for exploring transcriptional interactions. Bioinformatics 2008;24: 2636–8.
16. Zhang B, Horvath S. A general framework for weighted gene co-expression network analysis. Stat Appl Genet Mol Biol 2005;4:Article 17.
17. Gentleman RC, Carey VJ, Bates DM, Bolstad B, Dettling M, Dudoit S, Ellis B, Gautier L, Ge Y, Gentry J, et al. Bioconductor: open software development for computational biology and bioinformatics. Genome Biol 2004;5:R80.
18. Du P, Kibbe WA, Lin SM. lumi: a pipeline for processing Illumina microarray. Bioinformatics 2008;24:1547–8.
19. Storey JD, Tibshirani R. Statistical significance for genomewide studies. Proc Natl Acad Sci USA 2003;100:9440–5.
20. Benjamini Y, Hochberg Y. Controlling the false discovery rate—a practical and powerful approach to multiple testing. J R Stat Soc Ser B Stat Methodol 1995;57:289–300.
21. Thomas DE, Elliott EJ, Baur L. Low glycaemic index or low glycaemic load diets for overweight and obesity. Cochrane Database Syst Rev 2007;CD005105.

22. Márquez-Quiñones A, Mutch DM, Debard C, Wang P, Combes M, Roussel B, Holst C, Martinez JA, Handjieva-Darlenska T, Kalouskova P, et al. Adipose tissue transcriptome reflects variations between subjects with continued weight loss and subjects regaining weight 6 mo after caloric restriction independent of energy intake. Am J Clin Nutr 2010;92:975–84.
23. Kissebah AH, Vydelingum N, Murray R, Evans DJ, Hartz AJ, Kalkhoff RK, Adams PW. Relation of body fat distribution to metabolic complications of obesity. J Clin Endocrinol Metab 1982;54:254–60.
24. Mundi MS, Karpyak MV, Koutsari C, Votruba SB, O'Brien PC, Jensen MD. Body fat distribution, adipocyte size, and metabolic characteristics of nondiabetic adults. J Clin Endocrinol Metab 2010;95:67–73.
25. Arner E, Westermark PO, Spalding KL, Britton T, Ryden M, Frisen J, Bernard S, Arner P. Adipocyte turnover: relevance to human adipose tissue morphology. Diabetes 2010;59:105–9.
26. McMillan-Price J, Petocz P, Atkinson F, O'Neill K, Samman S, Steinbeck K, Caterson I, Brand-Miller J. Comparison of 4 diets of varying glycemic load on weight loss and cardiovascular risk reduction in overweight and obese young adults: a randomized controlled trial. Arch Intern Med 2006;166:1466–75.
27. Gardner CD, Kiazand A, Alhassan S, Kim S, Stafford RS, Balise RR, Kraemer HC, King AC. Comparison of the Atkins, Zone, Ornish, and LEARN diets for change in weight and related risk factors among overweight premenopausal women: the A TO Z Weight Loss Study: a randomized trial. JAMA 2007;297:969–77.
28. Rizkalla SW, Taghrid L, Laromiguiere M, Huet D, Boillot J, Rigoir A, Elgrably F, Slama G. Improved plasma glucose control, whole-body glucose utilization, and lipid profile on a low-glycemic index diet in type 2 diabetic men: a randomized controlled trial. Diabetes Care 2004; 27:1866–72.
29. Evans DJ, Hoffmann RG, Kalkhoff RK, Kissebah AH. Relationship of androgenic activity to body fat topography, fat cell morphology, and metabolic aberrations in premenopausal women. J Clin Endocrinol Metab 1983;57:304–10.
30. Dvoráková-Lorenzová A, Suchanek P, Havel PJ, Stavek P, Karasova L, Valenta Z, Tintera J, Poledne R. The decrease in C-reactive protein concentration after diet and physical activity induced weight reduction is associated with changes in plasma lipids, but not interleukin-6 or adiponectin. Metabolism 2006;55:359–65.
31. Nagy JA, Dvorak AM, Dvorak HF. VEGF-A and the induction of pathological angiogenesis. Annu Rev Pathol 2007;2:251–75.
32. Scroyen I, Jacobs F, Cosemans L, De Geest B, Lijnen HR. Effect of plasminogen activator inhibitor-1 on adipogenesis in vivo. Thromb Haemost 2009;101:388–93.
33. Ridker PM. High-sensitivity C-reactive protein: potential adjunct for global risk assessment in the primary prevention of cardiovascular disease. Circulation 2001;103:1813–8.
34. Gómez-Ambrosi J, Catalan V, Rodriguez A, Ramirez B, Silva C, Gil MJ, Salvador J, Fruhbeck G. Involvement of serum vascular endothelial growth factor family members in the development of obesity in mice and humans. J Nutr Biochem 2010;21:774–80.
35. Wycherley TP, Brinkworth GD, Keogh JB, Noakes M, Buckley JD, Clifton PM. Long-term effects of weight loss with a very low carbohydrate and low fat diet on vascular function in overweight and obese patients. J Intern Med 2010;267:452–61.
36. Lijnen HR. Angiogenesis and obesity. Cardiovasc Res 2008;78: 286–93.
37. Hoover-Plow J, Ellis J, Yuen L. In vivo plasminogen deficiency reduces fat accumulation. Thromb Haemost 2002;87:1011–9.
38. Romero MM, Fernandez-Lopez JA, Esteve M, Alemany M. Different modulation by dietary restriction of adipokine expression in white adipose tissue sites in the rat. Cardiovasc Diabetol 2009;8:42.
39. Rupnick MA, Panigrahy D, Zhang CY, Dallabrida SM, Lowell BB, Langer R, Folkman MJ. Adipose tissue mass can be regulated through the vasculature. Proc Natl Acad Sci USA 2002;99:10730–5.
40. Nishimura S, Manabe I, Nagasaki M, Hosoya Y, Yamashita H, Fujita H, Ohsugi M, Tobe K, Kadowaki T, Nagai R. Adipogenesis in obesity requires close interplay between differentiating adipocytes, stromal cells, and blood vessels. Diabetes 2007;56:1517–26.
41. Cao Y. Angiogenesis modulates adipogenesis and obesity. J Clin Invest 2007;117:2362–8.
42. Martinez-Hervas S, Romero P, Hevilla EB, Real JT, Priego A, Martin-Moreno JM, Carmena R, Ascaso JF. Classical cardiovascular risk factors according to fasting plasma glucose levels. Eur J Intern Med 2008;19:209–13.
43. Granata R, Trovato L, Lupia E, Sala G, Settanni F, Camussi G, Ghidoni R, Ghigo E. Insulin-like growth factor binding protein-3 induces angiogenesis through IGF-I- and SphK1-dependent mechanisms. J Thromb Haemost 2007;5:835–45.
44. Liu B, Lee KW, Anzo M, Zhang B, Zi X, Tao Y, Shiry L, Pollak M, Lin S, Cohen P. Insulin-like growth factor-binding protein-3 inhibition of prostate cancer growth involves suppression of angiogenesis. Oncogene 2007;26:1811–9.
45. Dawson DW, Volpert OV, Gillis P, Crawford SE, Xu H, Benedict W, Bouck NP. Pigment epithelium-derived factor: a potent inhibitor of angiogenesis. Science 1999;285:245–8.
46. Filleur S, Nelius T, de Riese W, Kennedy RC. Characterization of PEDF: a multi-functional serpin family protein. J Cell Biochem 2009; 106:769–75.
47. Wang P, Smit E, Brouwers MC, Goossens GH, van der Kallen CJ, van Greevenbroek MM, Mariman EC. Plasma pigment epithelium-derived factor is positively associated with obesity in Caucasian subjects, in particular with the visceral fat depot. Eur J Endocrinol 2008;159: 713–8.
48. Mutch DM, Tordjman J, Pelloux V, Hanczar B, Henegar C, Poitou C, Veyrie N, Zucker JD, Clement K. Needle and surgical biopsy techniques differentially affect adipose tissue gene expression profiles. Am J Clin Nutr 2009;89:51–7.